

Low-Reynolds-number predatorMehran Ebrahimiyan,¹ Mohammad Yekehzare,² and Mohammad Reza Ejtehadi^{3,*}¹*Department of Management and Economics, Sharif University of Technology*²*Department of Electrical Engineering, Sharif University of Technology*³*Department of Physics and Center of Excellence in Complex systems and Condensed Matter, Sharif University of Technology, Tehran, 1458889694, Iran*

(Received 26 November 2014; revised manuscript received 14 October 2015; published 31 December 2015)

To generalize simple bead-linker model of swimmers to higher dimensions and to demonstrate the chemotaxis ability of such swimmers, here we introduce a low-Reynolds predator, using a two-dimensional triangular bead-spring model. Two-state linkers as mechanochemical enzymes expand as a result of interaction with particular activator substances in the environment, causing the whole body to translate and rotate. The concentration of the chemical stimulator controls expansion versus the contraction rate of each arm and so affects the ability of the body for diffusive movements; also the variation of activator substance's concentration in the environment breaks the symmetry of linkers' preferred state, resulting in the drift of the random walker along the gradient of the density of activators. External food or danger sources may attract or repel the body by producing or consuming the chemical activators of the organism's enzymes, inducing chemotaxis behavior. Generalization of the model to three dimensions is straightforward.

DOI: [10.1103/PhysRevE.92.063035](https://doi.org/10.1103/PhysRevE.92.063035)

PACS number(s): 47.63.mf, 87.19.lu, 47.61.-k

The problem of swimming at a low Reynolds number is relevant to life on the microscale [1]. But swimming is not enough as the living cells should look for what they need. Although at a first glance the movement of a single-cell microorganism seems random, the ability to approach food resources or escape from hazards (chemotaxis) is essential for life [2,3]. Many simple and self-propelled microswimmers at low Reynolds numbers have been suggested [4–7]. To find how such swimmers can simulate a chemotaxis process, one should investigate the problem in more than one dimension.

Recently Najafi and Golestanian have introduced a simple swimmer and showed that it works well at low Reynolds number [8]. The swimmer consists of three solid beads contacting with two extensible tiny linkers in a line. The linkers change their length in a nonreciprocal but cyclic way. Because of the screening effect the viscous friction, applied to the beads by the fluid, depends not only on their speed but also on the distance between the beads. Thus the swimmer displacements do not cancel each others in a full period, and it swims. Simplicity of this swimmer makes it very interesting with the hope of construction of artificial swimmers [9], but life is not so simple. Cells are three-dimensional bodies with membrane walls.

Here we introduce a 2D variant of this low-Reynolds-number swimmer. The model again is constructed with three solid beads, with radius R , but connected by three arms with negligible thickness and length L , forming a triangle (Fig. 1). The triangular swimmer can easily be generalized to three dimensions in triangulated mesh membrane models [10].

The proposed swimmer is based on a chemical mechanism in which arms can change their length as a result of interaction with chemical substances in the environment. Interactions make the movement stochastic and result in random movement of the whole body with drift. Considering the symmetry of the

system, it is expected that the swimmer only moves in the plane of the triangle. Thus we call it a 2D swimmer.

There have been other attempts to introduce 2D and 3D swimmers [5–7,11]. Random movement of the swimmer in a low Reynolds number in a noisy environment has been reported ([12,13]). Also enhanced diffusion caused by reciprocal swimming [14] and stochastic swimming [15] are discussed in recent literature. However, our swimmer model shows chemotaxis behavior and could simply be generalized to three dimensions.

In the model swimmer, any linker of the triangle body may reduce its length from L to $(1 - \epsilon)L$ with a speed W or restore its original length with the same speed. For low Reynolds numbers, the nonlinear term of Navier-Stokes equation is negligible and the equation that describes the hydrodynamics of the swimmer in an incompressible flow condition, $\nabla \cdot \mathbf{u} = 0$, is $\mu \nabla^2 \mathbf{u} - \nabla p = 0$, where p and \mathbf{u} represent the pressure and velocity fields and μ denotes the fluid viscosity. Zero velocity at far distances, and a no-slip boundary condition on each sphere, are assumed, and the dynamical effects of the linkers on the swimmer's motion are neglected. Following Ref. [8] the linear form of the equations lets us find a relation between velocity of the sphere (\mathbf{V}_i) and the force applied to it (\mathbf{F}_i) as $\mathbf{V}_i = \sum_{j=1}^3 H_{ij} \mathbf{F}_j$, where H_{ij} is the symmetric Oseen tensor that depends on the geometry [11]. By considering Newton's laws and conservation of linear and angular momentums ($\sum \mathbf{F}_i = \mathbf{0}$ and $\sum \mathbf{r}_i \times \mathbf{F}_i = \mathbf{0}$), the set of equations are complete and can be treated numerically. The limited number of possible configurations of the body lets us solve the equations for any geometry once and save them to perform our simulations.

An advanced swimmer's movement can be explained by an ordered model in which arms open and close in a specific order. A full period of the cycle consists of six steps as shown in Fig. 1. Starting from a relaxed situation, in half of one cycle the linkers shrink in turn, and then they relax in the next half cycle in the same order. After a full cycle, the body

*ejtehadi@sharif.edu

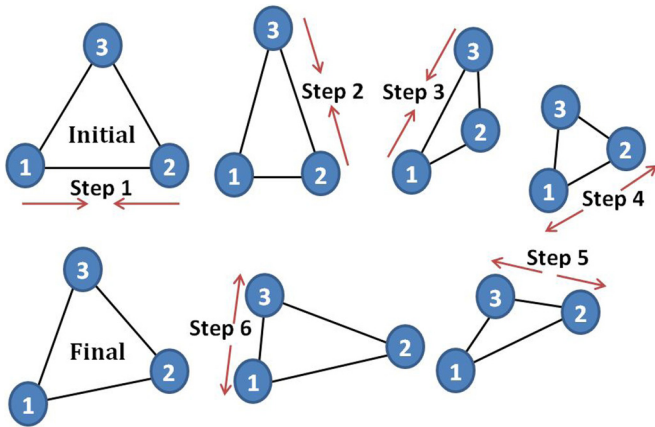


FIG. 1. (Color online) A full regular cycle started by contraction of one of the arms (e.g., arm 1–2 here) while the other arms follow it. After a half cycle they revert to their relaxed states in the same order. The last snapshot compares displacement of the swimmer after a full cycle with its initial position.

returns to its initial configuration but with a net displacement of the center of mass (COM) and a net rotation around it because of the hydrodynamic interactions between the balls. The total rotation and displacements of the body after a full cycle are shown in Fig. 2. If the swimmer keeps continuing its regular cycles, displacements in the end of the cycles are the same with just a constant rotation. Hence the swimmer’s COM completes a circular path of radius $\rho = |\bar{\Delta}|/\Delta\theta$ after $2\pi/\Delta\theta$ full cycles. The radius of the rotation [Fig. 2(b)] is smaller than R for possible values of ϵ , and much less than the size of the swimmer, L ; hence in this mechanism the swimmer rotates almost in place and acts as a fixed rotator.

However, it is quite probable that sources of randomness, e.g., thermal or chemical fluctuations, perturb our swimmer’s regular cycles. For example, we suppose that in the end of any

cycle the swimmer continues this cycle with a probability $(1 - p)$ or starts a new cycle with probability p which is different from the old one either in the cycle direction or in the starting arm. Therefore, the swimmer follows circular arcs which are kinked in points of perturbation. This introduces a very interesting run and tumble 2D walk which is composed of curved runs with 120° kinks in between (see Fig. 3). For $p \ll 1$ we can use a continuum approximation by introducing the rate of direction change $\eta = p/\Delta\theta$, which results in a diffusion coefficient $D = \omega\rho^2\eta/[2(1 + \eta^2)]$, where $\omega = \Delta\theta/\tau$ is the angular velocity of the swimmer along the arcs and $\rho = \Delta R/\Delta\theta$ is the radius of regular movement. Detailed calculations are presented in the Supplemental Materials [16]. As one expects for very small values of p the diffusion coefficient vanishes, because most of the time the swimmer acts like a fixed rotator and does not move far.

Similarly in the case of a linear swimmer (a swimmer alternatively switching the direction of its cycle), such noise results in a much more familiar random walk with 120° kinks and straight steps. As in the previous case, we suppose a probability p per cycle for a change in the swimmer direction, which results in $D = v^2\tau/2p^2$, where $v = \Delta R/\tau$ is the velocity of moving in a straight line. In this case the diffusion coefficient is a descending function of p in contrast to the first mechanism. The reason is that, whereas with the first mechanism the swimmer almost rotates in place and randomness helps it to move, in the latter mechanism the swimmer moves forward with a constant velocity, v , and randomness perturbs its directed motion.

The proposed model demonstrates a moving mechanism with a tendency for moving toward a particular direction. The proposed scenario may seem *ad hoc* without an unrealistic assumption; however, this idea can easily be modified to design a purposeful moving mechanism based on the physical foundations of the microworld. First, we will show that having a regular cycle after launching the first arm is not necessary for

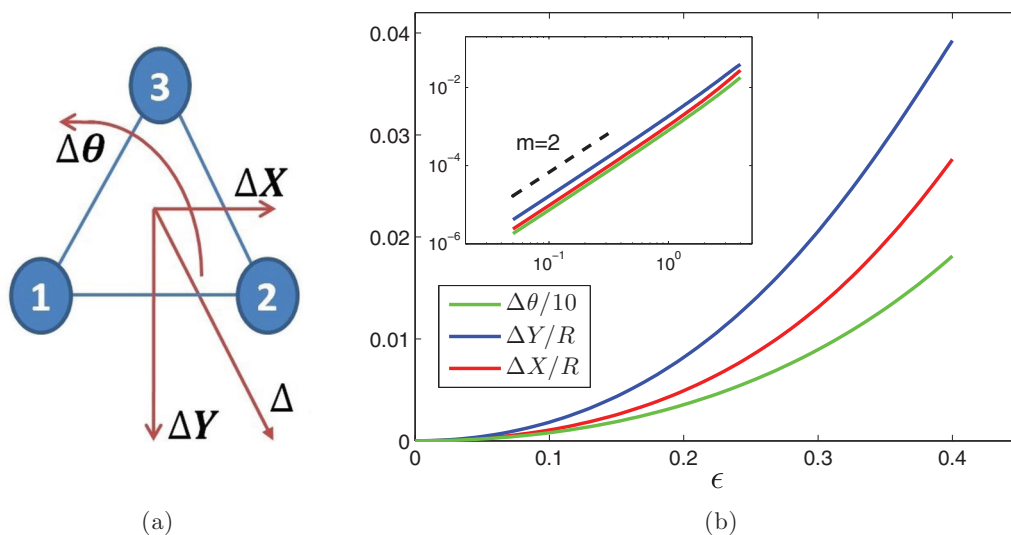


FIG. 2. (Color online) (a) After a full cycle, the body both rotates and moves. The movement, $\bar{\Delta}$, can be decomposed to the component parallel, ΔX , and perpendicular, ΔY , to the initial direction of the starter linker. (b) The displacements and rotations are shown for relaxed arm length $L = 10R$ as a function of contraction, ϵ . Inset shows the displacements in a log-log plot, which indicates that they are second order with respect to ϵ . The triangular geometry of the swimmer restricts ϵ to be not greater than $1/2$ (see intermediate steps in Fig. 1).

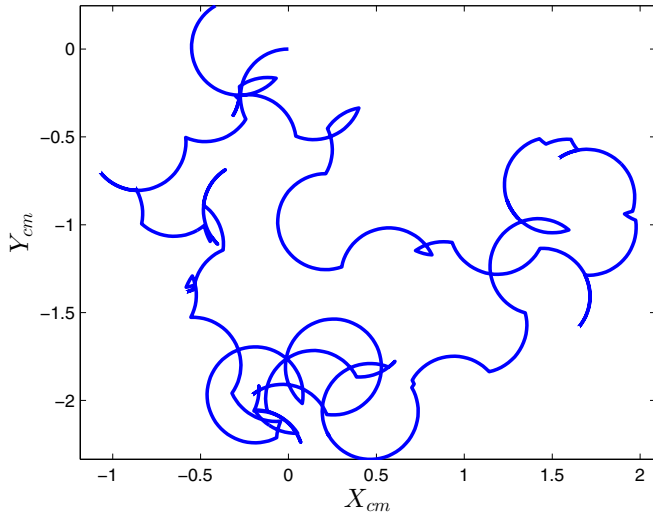
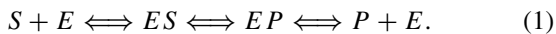


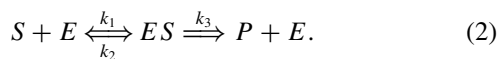
FIG. 3. (Color online) A typical path of the swimmer in 500 cycles for $L = 10$ and $\epsilon = 3$, which is perturbed by the probability $p = 0.1$. All the arcs have the same radius. The kinks are 120° because of the triangular symmetry of the swimmer. The arc lengths are random and have an exponential distribution.

moving in a specific direction. Second, we present a chemical mechanism for perturbing the probability of selecting arms: consider the situation in which micromachines, which are responsible for the change of the length of the linkers, are sensitive to the concentration of chemicals in their environment. For instance, we can assume the presence of some chemical nearby linkers that affect chemical equilibrium according to Le Châtelier’s principle: the probability of staying in the closed state for linkers, such as mechanochemical enzymes, may be dependent on the concentration of chemicals near that linker, and bonding with the linker results in expansion. In the case of space-varying concentration of activator chemicals, the transition rate between relaxed and contracted states of body arms is not symmetric, so the swimmer may be drifting to a particular high or low concentration zone.

We can assume that microchemical motors of arms act like enzymes, which we call E , and they can contribute microchemical reactions. It changes the substitute, S , to a final chemical product of P : the enzyme, E , combines with S and produces ES ; then ES becomes EP ; and finally, E takes apart from P :



ES and EP are states in which the enzyme has a different form from E ; we can assume that in states ES and EP the arm is open and in state E the arm is closed. These reactions are shown in Eq. (1). All the reactions are bilateral, but we can assume that transition from EP to $P + E$ is fast and one way because of the low concentration of P in the environment. Thus we can simplify the reaction with the given rates:



Transformation from $S + E$ to ES is also proportional to the concentration of S in the environment, c_s , so it is equal to $k_1 \cdot c_s$. Transformation ES to $S + E$ does not depend

on the concentration of S , thus it is equal to k_2 . Also the transformation of ES to $P + E$ does not depend on the concentration of chemicals and is just equal to k_3 . Thus we can find the probability of an arm remaining closed or open for time interval t as

$$p(t) = e^{-\frac{t}{\tau}}, \quad (3)$$

where τ is characteristic time of being in closed or open states, respectively. Here we conclude that t_o is constant,

$$t_o = \frac{1}{k_2 + k_3}, \quad (4)$$

and t_c depends on chemical concentration,

$$t_c = t_o \frac{k_m}{c_s}, \quad (5)$$

where $k_m = (k_2 + k_3)/k_1$.

Now we consider a given configuration for the swimmer with three links are numbered from 1 to 3, which may be in either open or closed state. Having the time constants of the transitions [Eqs. (4) and (5)], the probability that one of the links, e.g., number 1, changes its state before two others is given by

$$\frac{t_2 t_3}{t_1 t_2 + t_2 t_3 + t_1 t_3}, \quad (6)$$

where t_i is the time constant of i ’s arm that according to its state can be either t_o or t_c . Consider the case that c_s is equal to k_m , so that t_o is equal to t_c and the probability of choosing an arm is independent of the state and is equal to $\frac{1}{3}$. As well, if $c_s \gg k_m, t_o \gg t_c$, thus the closed arms are chosen sooner than the others for changing state, and after some transformation the body reaches the state in which all three arms are open; after that each arm is chosen to be closed by probability $\frac{1}{3}$, and if an arm is chosen to be closed, the same arm is chosen in the subsequent step to become open. On the other hand, in the case that $c_s \ll k_m, t_o \ll t_c$ and the open arms are chosen before the others, the system will reach the state in which all of the arms are closed; in this stage each of the arms is chosen to become open with equal probability, but the same arm will be selected for closing again. In both of the limit cases, after transitory steps, each state change for a given arm is quickly reversed, because of the tendency for being in a particular state. Hence, the consecutive state changes cancel each other out, because of the reversible feature of the microworld, and movement ability fails. Therefore, if the swimmer wants to move, c_s should be on the order of k_m . It means that the swimmer is designed to swim in a specific concentration.

Now consider a special case that the concentration of S, c_s is homogeneous in space, so the time constant of arms in each state is the same for all arms; by simulation, we have driven the diffusion coefficient as a function of $\frac{c_s}{k_m}$, depicted in Fig. 4. As discussed above, in the limits $c_s \ll k_m$ and $c_s \gg k_m$ the diffusion coefficient converges to zero. Also, there is an asymmetry in the figure between the diffusion coefficient in low and high concentrations. At low c_s , the time of an arm remaining closed is so large and the time of an arm remaining open is unchanged so that arms are mostly closed. In this case the average time between steps is t_c which is too large compared with t_o . On the other hand, at high c_s the time of an

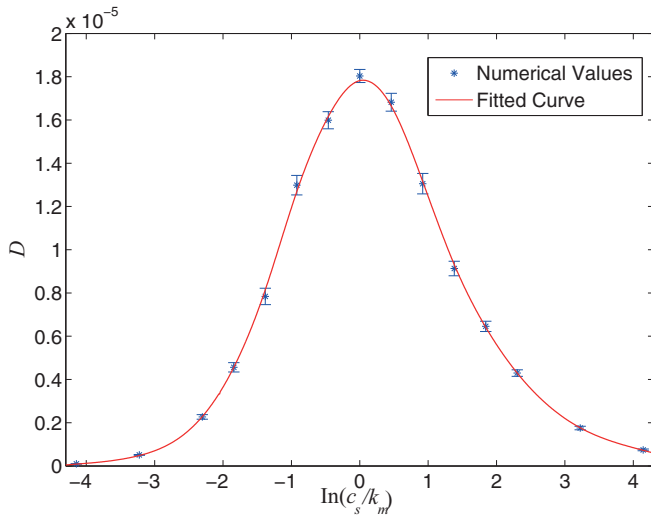


FIG. 4. (Color online) Diffusion coefficient is as function of $\log \frac{c_s}{k_m}$. The length of arm in the long state $L = 10R$ and the contraction ratio $\epsilon = 0.3$.

arm remaining closed becomes small and the time of an arm remaining open is unchanged, so in most times all arms are open; however, in this case the average time between steps is t_o , which is much less than the average time between steps in case low c_s . Therefore, the body moves more often than the case of low c_s , so the diffusion coefficient is larger.

In the previous discussion the concentration of activator substance, S , is assumed to be homogeneous in space; consider the case in which concentration is varying in space. In this case if all arms are open, because t_o is independent of concentration, the probability of changing states is the same, but when one or more of the arms are closed, the probability of changing state is different, so the symmetry of the movements is broken and the body may move to high or low concentrations, demonstrating a diffusion with drift.

In the first order of expansion with respect to concentration variation, the drift velocity can be written in the form $\mathbf{u} = f(c)\nabla \log(c)$, where c is the concentration of chemical activator and $f(c)$ determines the slope of drift with respect to environmental variations. Figure 5 plots the simulation results for $f(c)$. The unit of $f(c)$ is R^2/τ_o , where R is the radius of spheres and τ_o is expected time of an arm to stay relaxed. It can be seen again that in limit cases $c_s \ll k_m$ and $c_s \gg k_m$ the movement ability fails, because as discussed above, the consecutive state changes cancel out each other. The figure also shows an asymmetry similar to Fig. 4, which can be explained again by the fact that the time between steps is different in the two limit cases.

In the proposed model, the presence of chemicals adopts the preference of arms to be in their relaxed state. As a result, on average the swimmer moves towards the high concentration area, and it escapes the low concentration area. Thus the swimmer shows a perfect chemotaxis behavior. It approaches food resources when the closest arm to the food is more probable to revert to the restored state, and it escapes when the closest arm to the hazards prefers to be in the shortened or

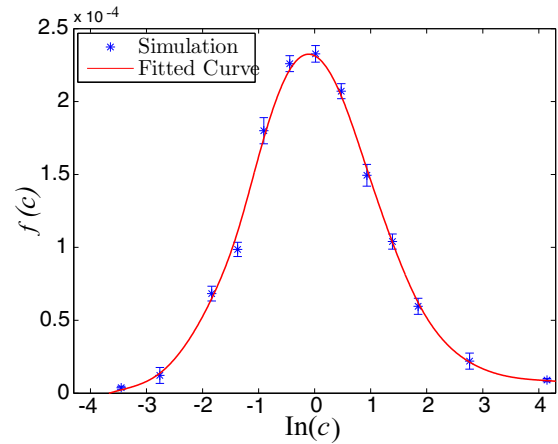


FIG. 5. (Color online) The average drift velocity response of a swimmer to variation slope of space-dependent concentration of chemical activators, as a function of concentration. For $c = 1$, expected time of being in a closed or open state for each arm is equal. Numerical results are based on enough number or time of simulations to reach precise average values.

relaxed state because of release or consumption of chemical stimulator by foods or dangerous objects.

To demonstrate this effect, we introduce a low-Reynolds predator-prey system. A tiny prey is swimming in the media. We assume that the hydrodynamic effect of the prey on the motion of the predator is negligible, but its metabolism somehow changes the chemistry of its environment in a way that our swimmer's (predator's) arms prefer to be in the relaxed state when the predator is close enough (to sense the chemistry). Figure 6 shows the geometry of our model predator and prey. The chemical concentration of environment is affected by the prey, which changes by $\frac{1}{r}$ in the environment, where r is the distance from the prey. The probability of changing the states of arms from closed and open states are

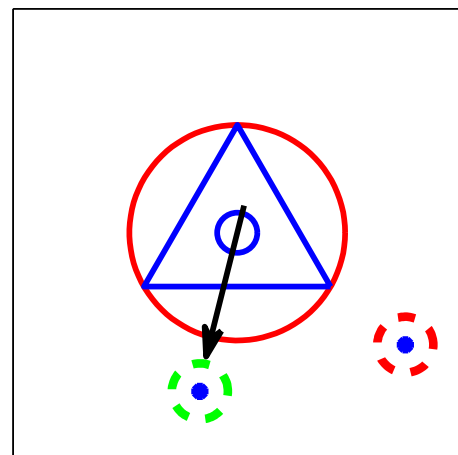


FIG. 6. (Color online) To introduce the predator it is supposed that the prey is a source of chemicals which affect the linkers' dynamics. The large red and small blue circles indicate the size and COM of predator, respectively. The arms of the predator swimmer are presented by blue triangles. The prey is the blue point with green circle.

simulated by the rules discussed in Eqs. (3) and (6). The movie in the Supplemental Material [16] shows how the swimmer chases its prey. In movie s1 the swimmer is chasing an escaping animal. The smaller body (prey) is doing a simple random walk and avoids the predator only with a simple hard core repulsive potential. It can be seen that the predator follows the prey with random perturbation showing the chemotaxis behavior.

Finally, it can be seen that extending the predator swimmer model to three dimensions is very straightforward. The simplest geometry is a tetrahedron of four spheres, connected by six arms. Again, each arm can change the length as in a 2D model. At any step one arm changes its state. The equations of motions are similar to the 2D case, and we should only solve a

bigger system of equations to find the spheres displacements. The translational and rotational displacements corresponding to this motion are smaller but still on the same order as the 2D swimmer, because the screening effect is weaker in the 3D case. Again, if we consider asymmetry in the rates of transitions, the chemotaxis effect on the motion of the swimmer is observed and can help it to move toward (or escape from) the sources of perturbations in 3D space.

We would like to thank Ali Najafi for very useful comments and his valuable suggestions, Ramin Golestanian for his fruitful discussions, and Nader Heydari for reading the draft manuscript and his valuable language comments.

-
- [1] E. M. Purcell, *Am. J. Phys.* **45**, 3 (1977).
 [2] H. C. Berg *et al.*, *Nature (London)* **239**, 500 (1972).
 [3] A. Bagorda and C. A. Parent, *J. Cell Sci.* **121**, 2621 (2008).
 [4] A. Shapere and F. Wilczek, *Phys. Rev. Lett.* **58**, 2051 (1987).
 [5] V. Lobaskin, D. Lobaskin, and I. M. Kuli, *Eur. Phys. J. Special Topics* **157**, 149 (2008).
 [6] J. E. Avron, O. Gat, and O. Kenneth, *Phys. Rev. Lett.* **93**, 186001 (2004).
 [7] B. U. Felderhof, *Phys. Fluids* **18**, 063101 (2006).
 [8] A. Najafi and R. Golestanian, *Phys. Rev. E* **69**, 062901 (2004).
 [9] M. A. Jalali, M.-R. Alam, and S. H. Mousavi, *Phys. Rev. E* **90**, 053006 (2014).
 [10] H. Noguchi, *J. Phys. Soc. Jpn.* **78**, 041007 (2009).
 [11] G. K. Batchelor, *J. Fluid Mech.* **74**, 1 (1976).
 [12] J. Dunkel and I. M. Zaid, *Phys. Rev. E* **80**, 021903 (2009).
 [13] R. Ledesma-Aguilar, H. Löwen, and J. M. Yeomans, *Eur. Phys. J. E* **35**, 70 (2012).
 [14] E. Lauga, *Phys. Rev. Lett.* **106**, 178101 (2011).
 [15] R. Golestanian and A. Ajdari, *J. Phys. Condens. Matter* **21**, 204104 (2009).
 [16] See Supplemental Material at <http://link.aps.org/supplemental/10.1103/PhysRevE.92.063035> for the detailed calculation of diffusion coefficient of random arc motion and also a movie which shows how a predator chases a prey which moves by a simple random walk and avoids predator with a simple hardcore repulsive motion.